Filomat 30:6 (2016), 1633–1650
DOI 10.2298/FIL1606633T

Published by Faculty of Sciences and Mathematics,
University of Niš, Serbia
Available at: http://www.pmf.ni.ac.rs/filomat

An Effective Approach for Evaluation of the Optimal Convergence Control Parameter in the Homotopy Analysis Method

Mustafa Turkyilmazoglu[a]

[a]*Department of Mathematics, Hacettepe University, 06532-Beytepe, Ankara, Turkey*

Abstract. A rapid and effective way of working out the optimum parameter of convergence control in the homotopy analysis method (HAM) is introduced in this paper. As compared with the already known ways of evaluating the convergence control parameter in HAM either through the classical $h-$level curves with h being the convergence control parameter or from the classical squared residual formula as adopted in the HAM society, an elegant way of calculating the convergence control parameter yielding the same optimum values is offered. In most cases, the new method is shown to perform quicker and better against the residual error method when integrations are much harder to evaluate or even by numerical means. Examples originating from real life applications selected from the literature demonstrate the validity and usefulness of the introduced technique.

1. Introduction

Ever since the development of the HAM by Liao in 1992 [4], more than a couple of thousand nonlinear mathematical models have been treated by researchers using HAM. A good collection of such problems, the power of the technique and its relation to already known approximate analytic methods were contained in the books [5] and [8].

It is now well-understood that the success of the HAM is constantly attributed to the so-called *convergence control parameter*, whose optimum value can be worked out making use of the traditional squared residual error definition after the work of [7], see also [3, 12, 13]. Desirable progress was also achieved on the convergence of HAM [9].

The present paper proposes a new way of finding out the optimum value of convergence control parameter used to ensure the convergence of the HAM series in a fastest manner, an idea first introduced in [9] (see chapter 5 in [9]). The proposed approach constitutes an alternative to both the classical h-level curves method and the squared residual error approach for determination of optimal value of the convergence control parameter. It is demonstrated through examples from the open literature that the squared residual error method and the present one generate nearly identical optimal convergence control parameter values, even though less computational cost is the advantage of the presented scheme. Not only the optimum value of the convergence control parameter is obtained via the new method, but also the interval of convergence can be gained and the guarantee of quick convergence can be given.

2010 *Mathematics Subject Classification*. 34Axx; 35Axx; 37Axx; 39Axx; 41Axx; 45xx; 76Axx
Keywords. Homotopy analysis method, Convergence control parameter, h-curve, Squared residual approach, Ratio approach
Received: 11 May 2014; Accepted: 13 December 2014
Communicated by Dragan S. Djordjević
Email address: turkyilm@hacettepe.edu.tr (Mustafa Turkyilmazoglu)

2. Traditional Ways and the Presently Proposed Approach

The layout of the HAM is now well-documented in the literature and hence will be omitted here for the conciseness, anyway, the interested readers may refer to the very recent book [9]. To be more precise, it is intended to construct a homotopy of the form

$$(1-p)\mathcal{L}[u(t,p)-u_0(t)] - p\,h\,H(t)\mathcal{N}[u(t,p)] \quad = \quad 0, \tag{1}$$

to a nonlinear problem $N(u,t)=0$, where $p\in[0,1]$ is *the homotopy embedding parameter*, h is *the convergence control parameter* adjusting the convergence, $\mathcal{L}$ is a selected linear operator, $u_0(t)$ is an initial guess for wanted solution $u(t)$, $H(t)$ is an auxiliary function. Upon adequate number of successive differentiations of (1), the following homotopy series is reached

$$u(t) \quad = \quad u_0(t) + \sum_{k=1}^{\infty} u_k(t), \tag{2}$$

which was proved by Liao [5] to correspond to the exact solution desired.

By truncating the homotopy series (2), eventually *an approximate analytic solution of Mth-order* for a physical problem of interest can be represented by

$$u_M(t) \quad = \quad u_0(t) + \sum_{k=1}^{M} u_k(t), \tag{3}$$

whose limiting value

$$\lim_{M\to\infty} u_M(t)$$

leads to the *the exact solution* $u(t)$.

Based on a sufficient theorem to ensure the convergence of homotopy series (2), a novel approach was outlined [9] (see chapter 5 in [9]), which is restated in the following Corollary

Corollary 2.1. *For a preassigned value of h, for convergence of the homotopy series (2) it is sufficient to keep track of magnitudes of the ratio β defined by*

$$\beta \quad = \quad \frac{\|u_{k+1}(t)\|}{\|u_k(t)\|}, \tag{4}$$

and to check whether it remains less than unity for increasing values of k. An optimal value for the convergence control parameter h could also be determined from (4) by requiring the ratio β to be as close to zero as possible, so that for such a value the rate of convergence of homotopy series (2) will be the fastest, since then the remainder of the series will most rapidly decay.

Moreover, in the case of a preassigned value h of the convergence control parameter, when the absolute value norm is chosen, the region of t for the wanted solution can also be identified. Additionally, the ratio given in (4) can also plot the constant h-curves [5] correctly. Furthermore, on the condition that one is concerned with the zeros of equation $f(x)=0$ of the algebraic kind, the inequality

$$\frac{|x_{k+1}|}{|x_k|} < 1 \tag{5}$$

for large k produces the convergence control parameter interval.

In place of the constant $h-$level curves, the norm defining the residual

$$Res(h) \quad = \quad \|\mathcal{N}[\sum_{k=0}^{M} u_k(t)]\|,$$

where the norm is in the sense L^p, with $p = 2$ in general [16], the subsequent squared residual error is often employed to determine an optimal h

$$Res(h) = \int_A \left\{ \mathcal{N}\left[\sum_{k=0}^{M} u_k(r) \right] \right\}^2 dr, \tag{6}$$

for which the physical problem takes place over the set A. In the case of a positive integrand, the residual error in (6) can be replaced by

$$Res(h) = \int_A \mathcal{N}\left[\sum_{k=0}^{M} u_k(r) \right] dr, \tag{7}$$

based on L^1 norm to gain more computational time. We should mention here that following [7], the discrete forms corresponding to (6) and (7) may be suggested

$$Res(h) \approx \frac{1}{N+1} \sum_{j=0}^{N} \left\{ \mathcal{N}\left[\sum_{k=0}^{M} u_k(t_j) \right] \right\}^2, \tag{8}$$

$$Res(h) \approx \frac{1}{N+1} \sum_{j=0}^{N} \mathcal{N}\left[\sum_{k=0}^{M} u_k(t_j) \right]. \tag{9}$$

with equally distributed N discrete points. By requiring from (6), (7), 8 or (9) that

$$\frac{dRes(h)}{dh} = 0, \tag{10}$$

optimal values of the convergence control parameter h for a nonlinear physical problem can be determined.

The main disadvantages of the residual are that exact integration from (6) and (7) may not be clear or computational cost of discrete forms (8) or (9) may not be at the expense of desire, particularly for the unbounded physical problems. Owing to such shortcomings, by means of the ratio given in equation (4), a novel and easy way of finding h was suggested in [9] by letting the ratio β in (4) to be sufficiently small. If possible then *the optimums of the convergence control parameter h* might be as a consequence of

$$\frac{d\beta}{dh} = 0,$$

or at worst, graphs of constant $\beta-$curves will play the role of determining an optimal value of h in (4). Therefore, in line with [9],

$$\beta = \frac{\int_A u_{k+1}^p(r)dr}{\int_A u_k^p(r)dr}, \tag{11}$$

or its discrete counterpart

$$\beta \approx \frac{\sum_{j=0}^{N}[u_{k+1}(t_j)]^p}{\sum_{j=0}^{N}[u_k(t_j)]^p}, \tag{12}$$

will serve good to get the optimum convergence control parameter h.

It is noted that whenever exact solution or numerical estimation $u_e(t)$ is at our disposal for a considered problem, the absolute error

$$err = \int_A |u_e(t) - u(t)|dt \tag{13}$$

may be employed to check the accuracy of homotopy solution $u(t)$ as obtained from (3).

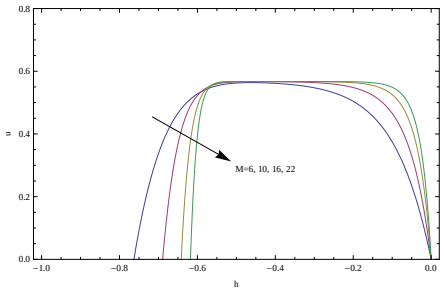

Figure 1: $h-$level curves for equation (14).

3. Examples

In order to test the new approach and its validity through the utilities (6–12) (refer also to chapter 5 in [9] for further analysis), some physical problems are considered here collected from various homotopy analysis research in the open literature.

3.1. A transcendental equation

Our first example is the transcendental equation

$$f(u) = ue^u - 1 = 0, \tag{14}$$

whose numerical solution up to ten significant digits is simply $u = 0.5671432904$. The choices

$$u_0 = 0, \qquad \mathcal{L}(u) = f(u) - f(u_0)$$

helps us to construct the homotopy series solution via the homotopy approach (1) from the residual and absolute errors

$$Res(h) = ue^u - 1, \tag{15}$$

$$err = u - \text{ProductLog}[1]. \tag{16}$$

It is computed from (15) that the $22th$-order approximation $h = -0.44$ yields the minimum value for the residual.

Figure 1 clearly demonstrate that the interval of convergence for h is $h \in [-0.6, 0)$. Indeed, from (5) by analytically solving the inequality $|u_{22}/u_{21}| < 1$, we find $-0.55721 < h < 0$. At the above calculated value of $h = -0.44$, Table 1 gives the root and the absolute error (15) and also the result using the classical algorithm of modified Newton iteration (see [8])

$$u_k = u_{k-1} + h\frac{f(u_{k-1})}{f'(u_{k-1})}. \tag{17}$$

From Table 1 it is understood that $h = -0.44$ is good enough for the homotopy analysis method, as verified also from Table 2, even surprisingly better convergent HAM solutions are obtained than the Newton method. Tables 2-3 and Figures 2 (a–b) are clear evidences that as M tends to infinity, the optimums computed from the residual using (15) and the ratio with (5) will be equal.

The ratio (5) can also be assessed from Figure 3 and Table 4 corresponding to the optimum convergence control parameter $h = -0.423$. The insurance of convergence is due to the less than unity value of β which actually limits to 0.57634. It is also observed that to find the minimum values of (15) for $M = 151$, 201, 251 and 351, respectively 40, 70, 110 and 926 seconds are needed, whereas only 5, 14, 36 and 82 seconds are sufficient for evaluating minimums from (5). This obviously points to advantageous CPU time for the present approach.

M	5	10	15	20
u^{a}	0.5612802859	0.5668842143	0.5671363654	0.5671427617
err^{a}	5.8630×10^{-3}	2.5908×10^{-4}	6.9250×10^{-6}	5.2870×10^{-7}
u^{b}	0.5566418620	0.5665732963	0.5671119237	0.5671415630
err^{b}	1.0501×10^{-2}	5.6999×10^{-4}	3.1367×10^{-5}	1.7274×10^{-6}

Table 1: Zeros of (14) and absolute errors for some M at $h = -0.44$. [a]Solutions from homotopy (3) and [b]Solutions from Newton iteration (17).

M	10	20	30	50	100	200	300	350
h	-0.4501	-0.4392	-0.4350	-0.4312	-0.4280	-0.4262	-0.4255	0.4253

Table 2: The resulting values of optimum for h using the ratio (5) and residual (15).

M	21	51	101	151	201	251	301	351
h^{a}	−0.4455	−0.4341	−0.4295	−0.4278	−0.4270	−0.4264	−0.4260	−0.4257
h^{b}	−0.4074	−0.4162	−0.4196	−0.4209	−0.4216	−0.4220	−0.4223	−0.4225
β	0.57160	0.57523	0.57604	0.57621	0.57626	0.57628	0.57629	0.57629

Table 3: The values of optimal h and ratio β. [a]Equation (15) and [b]Equation (5).

M	100	150	200	300	400	460	490	500
β	0.59136	0.58438	0.58082	0.57771	0.57667	0.57643	0.57636	0.57634

Table 4: The values of ratio β with $M = 500$ and $h = -0.423$.

3.2. *A nonlinear differential-difference equation of Volterra type*

The next example is the famous nonlinear Volterra differential-difference initial value problem

$$u_n'(t) = u_n(t)(u_{n-1}(t) - u_{n+1}(t) + u_{n-2}(t) - u_{n+2}(t)), \quad u_n(0) = n, \quad 0 \le t \le 1, \tag{18}$$

whose physical importance was highlighted in [8]. The exact solution was given in the study [18] as $u_n(t) = \frac{n}{1+6t}$.

By means of selecting, respectively,

$$H(t) = 1, \quad \mathcal{L} = \frac{d}{dt}, \quad u_{n,0}(t) = n - t,$$

the inequality outlined in (5) for $u_{10}'(0)$ gives rise to the the interval $[-2,0]$ h, which is also depicted from the h-level curves in Figure 4.

Carrying out the numerical integration for the residual (with 500 equal points) and exact integration for the ratio at $n = 10$, it is seen from Figures 5 (a–b) and Table 5 that the residual (8) and the ratio (11) (with $p = 2$) generate nearly the same region of convergence, both limiting towards the optimal value $h = -0.245$. The fast convergence via the present ratio approach is also apparent, see also plot of the ratio β in Figures 6 (a–c).

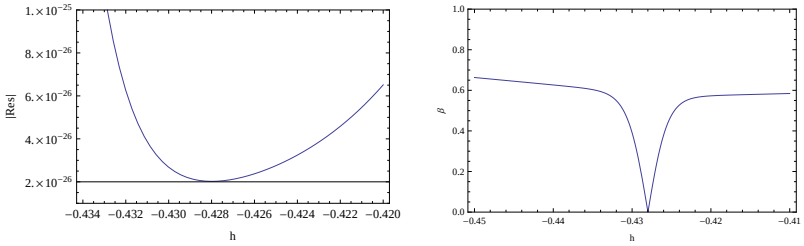

(a) The tesidual error (b) The ratio approach

Figure 2: The error $|Res|$ and the ratio β regarding the problem (14) for the approximation level $M = 301$.

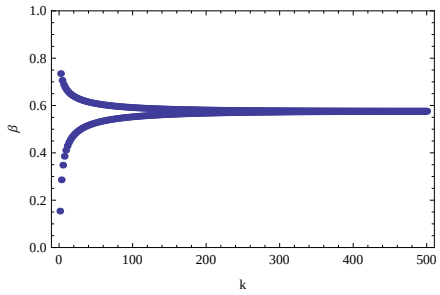

Figure 3: The ratio β for equation (14).

M	10	20	30	40	50
h^{a}	−0.2292(17)	−0.2365(44)	−0.2398(83)	−0.2417(124)	−0.2430(200)
h^{b}	−0.2269(4)	−0.2374(9)	−0.2417(16)	−0.2440(26)	−0.2453(43)
β	0.20876	0.24327	0.28104	0.30947	0.33092

Table 5: The optimal h and β values for equation (18) (with CPU times in parenthesis). [a] From equation (8) and [b] From equation (11).

3.3. *A nonlinear first-order Fredholm integro-differential equation*

Let us consider the subsequent strongly nonlinear Fredholm integro-differential equation of first-order

$$u'(t) + u(t) + \int_0^t u^2(x)dx = \frac{1}{2}\left(1 - e^{-2t}\right), \quad 0 < t < 1, \tag{19}$$

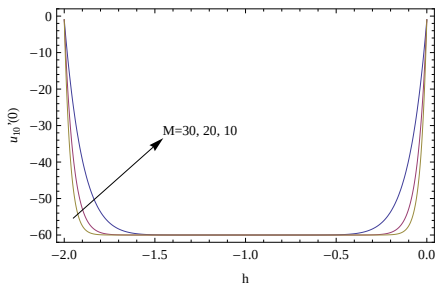

Figure 4: h-level curves for equation (18).

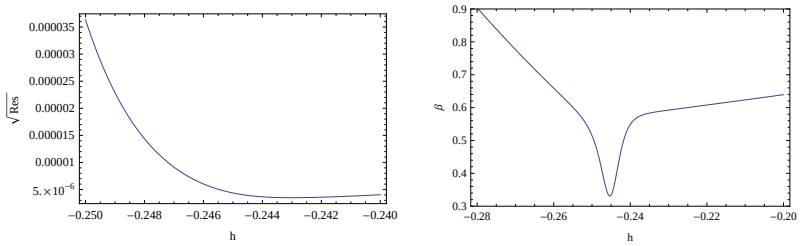

(a) The residual error (b) The ratio approach

Figure 5: The error $\sqrt{Res}$ and the ratio β regarding the problem (18) for the approximation level $M = 50$.

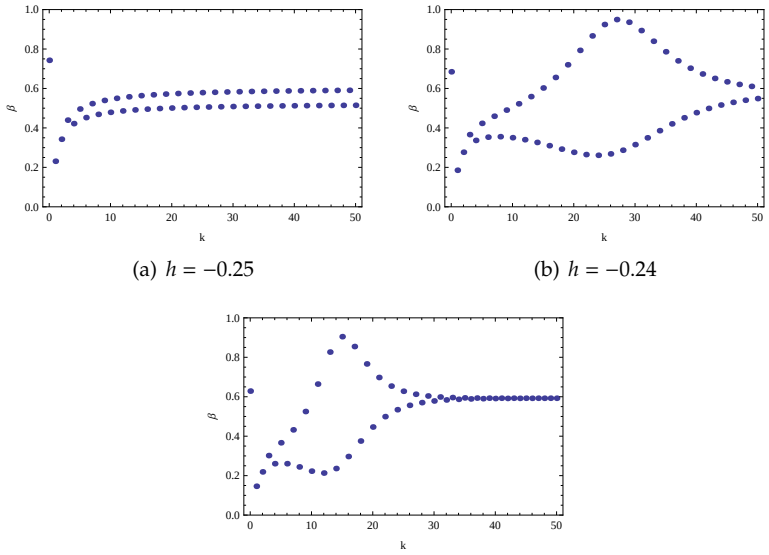

(a) $h = -0.25$ (b) $h = -0.24$

(c) $h = -0.23$

Figure 6: The ratio β for equation (18).

whose initial condition is supplemented by

$$u(0) = 1. \tag{20}$$

The exact solution is given by $u_e(t) = e^{-t}$ and the HAM approach involves the auxiliary parameters

$$\mathcal{L} = \frac{d}{dt}, \quad u_0(t) = 1.$$

Figure 7 is for the constant h–curves showing that the interval is [-2,0] for the convergence control parameter. This interval was also worked exactly for $u'(0)$ from the inequality (4) at the approximation orders mentioned in figure 7.

Because the exact integration of the squared residual (6) takes longer, the minimization was implemented through the discrete version (8) for the residual using 100 equally spaced points. However, the ratio is still obtained from (11) and does not require any discrete integration. The optimal value from both approaches is again limiting to the same value of $h = -0.85$, and the better character of the present approach is clear from Figures 8 (a–b) and Table 6. Figure 9 also reveals how the ratio β makes the HAM convergent for the present problem.

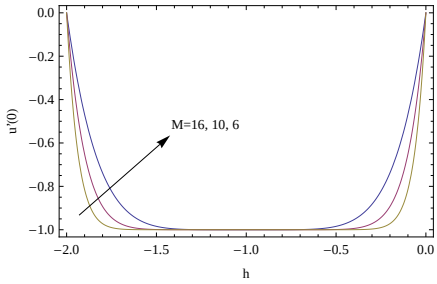

Figure 7: h-level curves for equation (19).

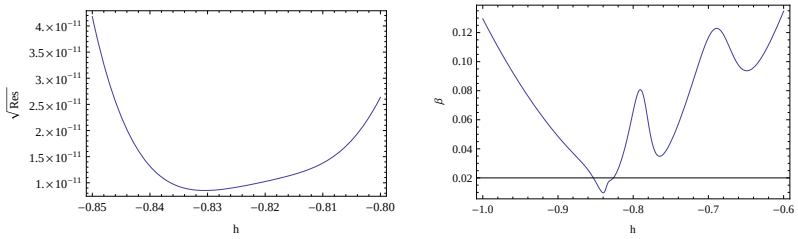

(a) The residual error (b) The ratio approach

Figure 8: The error $\sqrt{Res}$ and the ratio β regarding the problem (19) for the approximation level $M = 15$.

M	1	5	7	11	15
h^{a}	−0.5408(4)	−0.7923(35)	−0.7998(66)	−0.8266(120)	−0.8305(145)
h^{b}	−0.6376(1)	−0.7110(3)	−0.8250(6)	−0.8227(21)	−0.8398(38)
β	0.06009	0.03641	0.01301	0.01130	0.00972

Table 6: The values of optimal h and β for equation (19) (with CPU times in parenthesis). [a] From equation (8) and [b] From equation (11).

3.4. *Mixed convection flow*

Consider now steady mixed convection flow past a plane of arbitrary shape under the boundary layer and Darcy-Boussinesq approximations [10], governed by the second-order nonlinear differential equation

$$2u'' + u - u^2 = 0, \quad u(0) = 0, \quad u(\infty) = 1. \tag{21}$$

With the choices of

$$\mathcal{L} = \frac{d^2}{dt^2} - 1, \quad u_0(t) = 1 - e^{-t}, \quad H(t) = 1,$$

figure 10 shows $u'(0)$ and the interval of convergence control parameter h associated with it. A better prediction is obtained via the relation (4) generating the whole interval [−1.008,0] from the 31th-order homotopy series approximation.

It is remarked here that it was almost impossible to get the exact residual over the semi-infinite domain, so discrete version is used. However, exact integration is still carried out for the ratio. With $M = 30$ number of homotopy terms, the discrete squared residual and exact ratio are found to produce a minimum around $h = -0.81$ as seen from Table 6 and Figures 11(a)-11(b).

Figure 12 and 13 are further evidences that $h = -0.8$ accomplishes the convergence of the homotopy series.

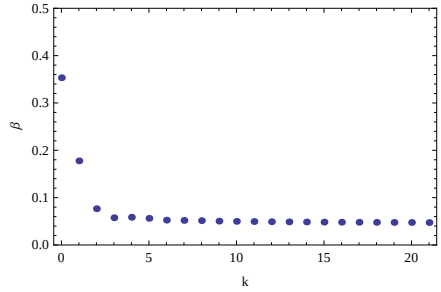

Figure 9: The ratio β for equation (19).

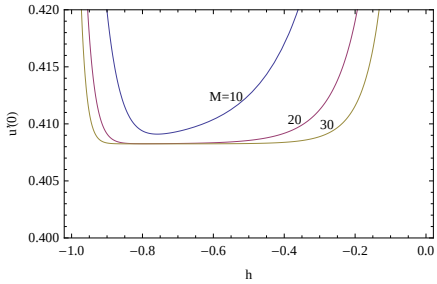

Figure 10: $h-$level curves for equation (21).

M	6	10	20	26	30
h^{a}	−0.7333	−0.7640	−0.7969	−0.8066	−0.8113
h^{b}	−0.7260	−0.7611	−0.7975	−0.8078	−0.8128

Table 7: The values of optimal h and β for equation (19). [a] From equation (9) and [b] From equation (11).

3.5. Vibration of Von Karman rectangular plates

The highly nonlinear second-order non-damped vibration equation

$$u'' + u + u^3 + u^2u'' + uu'^2 = 0, \quad u(t=0) = A, \quad u'(t=0) = 0, \tag{22}$$

models the equations of motion for a rectangular isotropic plate, considering the effect of shear deformation and rotary inertia from the Von Karman theory [11], with amplitude of the oscillations is represented by A which is set to unity. Using a suitable transformation $t = \omega\,\tau$ and considering that $1/\omega$ denotes frequency of the oscillations, equation (22) becomes

$$u'' + \omega^2(u + u^3) + u^2u'' + uu'^2 = 0, \quad u(0) = A, \quad u'(0) = 0. \tag{23}$$

We employ the subsequent variables

$$u_0(\tau) = A\cos\tau, \quad \mathcal{L} = \frac{d^2}{d\tau^2} + 1, \quad H(\tau) = 1,$$

$$\omega = \sum_{i=0}^{\infty} \omega_i$$

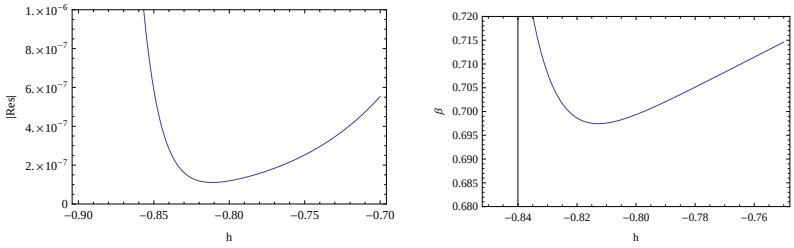

(a) The residual error (b) The ratio approach

Figure 11: The error $|Res|$ and the ratio β regarding the problem (21) for different levels of approximation M.

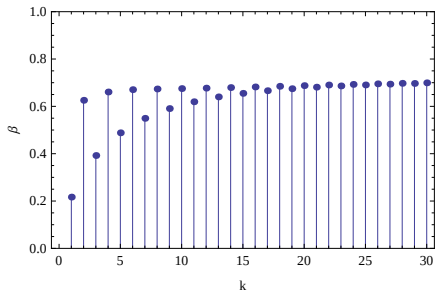

Figure 12: The ratio β for equation (21).

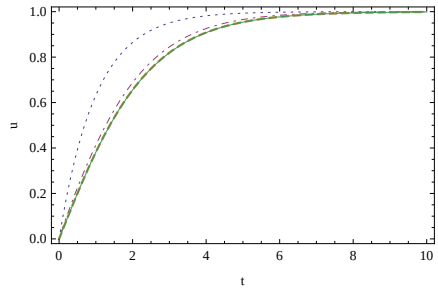

Figure 13: Solution of equation (21). Full solution (solid curve); 10th-order HAM approximation (dashed curve); 3th-order HAM approximation (dashed-dotted curve) and initial approximation (dotted curve).

and make use of the HAM approach as in [14] after further rescaling the convergence control parameter as $\frac{h}{\omega_0^2}$.

Figures 14 (a–b) exhibit the convergence interval as a consequence of evaluating the physical variables $u''(0)$ and ω. The convergence interval appears to be $[-1,0]$ from these figures, which was also analytically justified; an exact interval of $[-0.8585,0]$ was obtained using (4) for $u''(0)$ and the interval of $[-0.8897,0]$ using (5) for ω at the homotopy approximation level $M = 26$. At this level, Table 8 tabulates the frequency and absolute residual error for the optimal value corresponding to $h = -0.58$. As the approximation level gets higher, the frequency is better estimated as a result of rapidly decaying absolute residual error.

With the choice of $h = -0.6$, the ratios (4) for u and (5) for ω as shown in Figures 15 (a–b) further justify the converge of the HAM solution to the true oscillator problem. Figures 15(a-b) also indicate that the ratio of ω will suffice to determine the convergence, avoiding the heavy integrations during the evaluation of squared residuals errors signifying the considerable advantage of the present approach as also tabulated in in Table 9 while finding the optimum value for h by means of minimization of the ratio (5) associated with

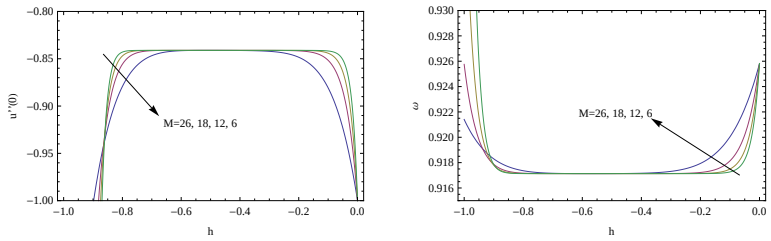

(a) $u''(0)$ against h (b) ω against h

Figure 14: h-level curves for equation (23).

M	6	12	18	26
ω	0.9171342221	0.9171341643	0.9171341646	0.9171341646
Res^{a}	7.5705×10^{-2}	7.4089×10^{-5}	9.0351×10^{-8}	1.4349×10^{-11}

Table 8: Taking $A = 1$ when $h = -0.58$, HAM solutions are tabulated for ω and resulting Res concerning the problem (23). [a]Equation (7).

ω.

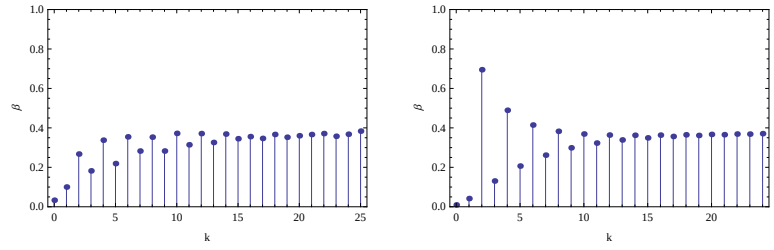

(a) β for ω (b) β for u

Figure 15: The ratio β for equation (23) by means of $h = -0.60$.

M	5	9	15	21	25
h	-0.57391	−0.57244	−0.57179	−0.57159	−0.57153

Table 9: Minimizing the ratio (5) associated with ω and the resulting optimal h values.

The above analysis is also verified in Figures 16 (a–b) Table 10, which are computed by taking [0,2π] as the domain of integration in (23), see [8].

Finally, the uniform convergence of HAM as used for the current model is shown in Figures 17 (a–d)evaluated at $h = -0.6$. It is seen that a large domain is truly estimated by the HAM.

3.6. A nonlinear high-order eigenvalue problem

Let us consider now the strongly nonlinear eigenvalue problem (see, page 340 in [8])

$$\begin{aligned} \lambda u'''' - \beta t(1 + \lambda^2 u^2) &= 0, \\ u(0) = u'(1) = u''(1) &= u''(0) - u''(\alpha) = u(1) - 1 = 0, \end{aligned} \tag{24}$$

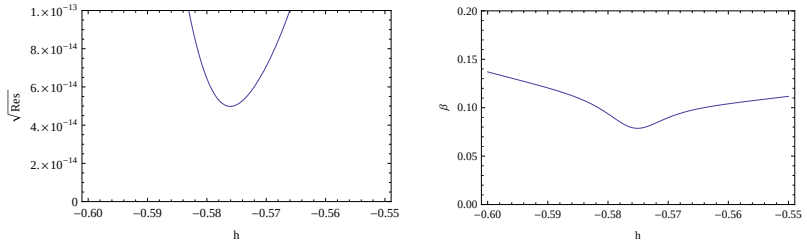

(a) The residual error (b) The ratio approach

Figure 16: The error $\sqrt{Res}$ and the ratio β regarding the problem (23) for the level of approximation $M = 20$.

M	h^{a}	CPU times	h^{b}	β	CPU times
3	−0.58254	11	−0.58476	0.03073	4
5	−0.58312	48	−0.58159	0.04423	9
11	−0.57968	106	−0.57771	0.06390	24
15	−0.57823	146	−0.57656	0.07031	38
19	−0.57724	187	−0.57582	0.07453	53
25	−0.57605	331	−0.57508	0.07873	73

Table 10: The optimal h values, β values and the CPU times in seconds for equation (23) for various M. [a]Equation (8) and [b]Equation (12).

where λ is an eigenvalue, the last condition is the normalizing condition and we fix $\alpha = 1/5$ and $\beta = 10$ to comply with [8].

A treatment of the nonlinear eigenvalue problem (24) was presented in [8] and so we closely follow that source in our HAM approach. In line with [8], the eigenvalue is $\lambda = 0.6273146267$ and the following variables are under consideration during the HAM procedure

$$u_0(t) = \frac{1}{2\alpha - 3}\left(2(3\alpha - 4)t + 6(1-\alpha)t^2 + 2\alpha t^3 - t^4\right), \quad \mathcal{L} = \frac{d^4}{dt^4}, \quad H(t) = 1.$$

Figures 18 (a–b) reveal the constant $h-$curves of $u'(0)$ and λ for changing approximation levels, which result from 6th-order of approximation via the ratios (4) from $u'(0)$ as

$$[-2.9128, 0), \quad [-2.77459, 0),$$

and from 10th-order approximation via (5) from λ as

$$[-2.8508, 0), \quad [-2.74587, 0),$$

respectively.

Using 40 points during the numerical treatment, Figures 19 (a–b) reveal the squared residual error and λ. From these figures we can deduce that both yields nearly the same value of $h = -1.5$, whose exact values are also given in Table 11. We should note that integration for the squared residual even with so coarse grid took about 10 minutes, whereas only 2 seconds were enough for the ratio of λ, which illustrates the power of the ratio approach introduced.

The accuracy and convergence of the HAM approximations for the present model are evident after the ratio β as revealed in Fgures 20 (a–c).

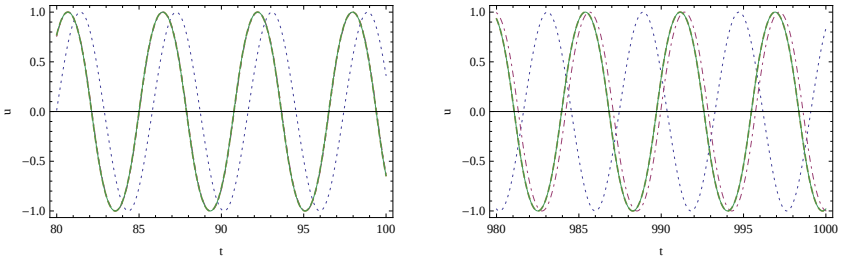

(a) For $t \in [80, 100]$ (b) For $t \in [980, 1000]$

(c) For $t \in [9980, 10000]$ (d) For $t \in [29980, 30000]$

Figure 17: Views for the non damped rectangular plate problem (22). Full solution (unbroken curve); 6th-order homotopy approximation (dashed curve); 2nd-order homotopy approximation (dashed-dotted curve); initial approximation (dotted curve).

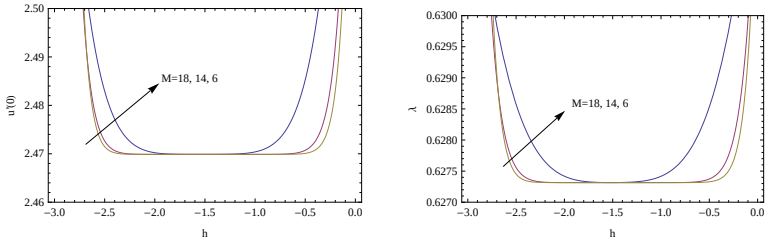

(a) h-level curves for $u'(0)$ (b) h-level curves for λ

Figure 18: h-level curves for equation (24).

M	3	5	9	13	17
λ	0.6273673927	0.6273155785	0.6273146272	0.6273146267	0.6273146267
h^{a}	-1.520677996	-1.520314185	-1.519994824	-1.519845133	-1.519756991

Table 11: Values of λ and optimum h for various M for equation (24). [a]Equation (5).

3.7. A nonlinear system modelling the HIV infection of $CD4^+$ T-cells

We now consider the model for HIV infection of $CD4^+$ T-cells of Culshaw and Ruan [1] (see also [2])

$$\begin{cases} T'(t) &= s - \mu_T T + rT\left(1 - \frac{T+I}{T_{max}}\right) - k_1 VT, \\ I'(t) &= k_2 VT - \mu_1 I, \\ V'(t) &= N\mu_b I - k_1 VT - \mu_V V, \end{cases} \tag{25}$$

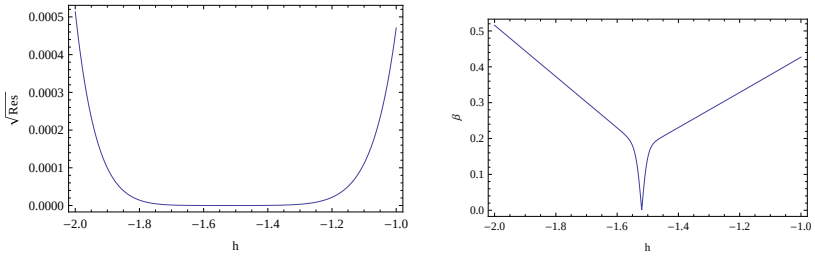

(a) The residual error (b) The ratio approach (for λ)

Figure 19: The error $\sqrt{Res}$ and the ratio β regarding the problem (24) for the level of approximation $M = 18$.

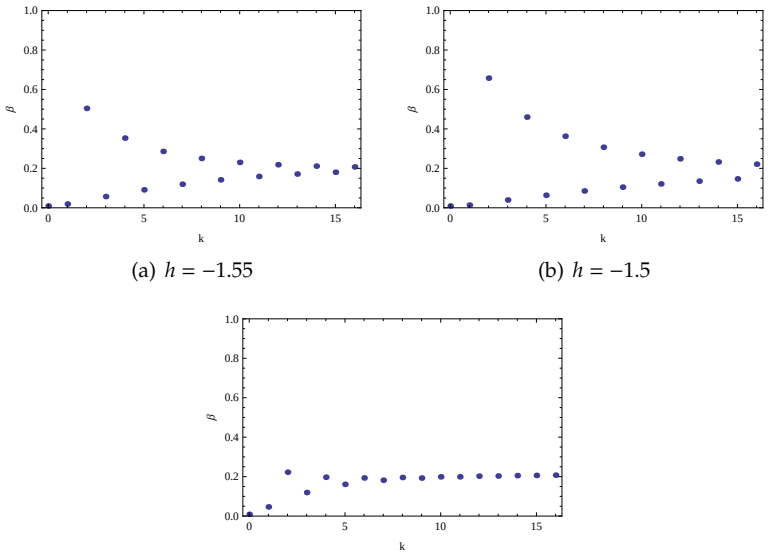

(a) $h = -1.55$ (b) $h = -1.5$

(c) $h = -1.45$

Figure 20: The ratio β for λ for equation (24).

which was developed to describe infection by the human immunodeficiency virus (HIV). Here $T(t)$, $I(t)$ and $V(t)$ represent the concentration of healthy CD4$^+$ T-cells at time t, infected CD4$^+$ T-cells, and free HIV at time t, respectively. Further explanations on the variables, parameters and initial conditions can be found in [2]. In line with [2], we make use of

$$\mathcal{L} = \frac{d}{dt}$$

as the auxiliary linear operator and also we take the same convergence control parameter h for the three differential equations in system (25). We should note that [2] contains the HAM solutions only within a limited time period $t \in [0, 1]$, but we extend it to any desired time span $t \in [0, t_m]$, where we take $t_m = 10$ for the present study. Moreover, the convergence analysis of the HAM applied to the model (25) was given in [2] only in terms of squared residuals.

Figures 21(a–b) display the h-level curves of $T'(0), I'(0)$ and $V'(0)$ with $M = 60$. The interval $[-2, 0]$ is seen to be proper domain of convergence of the HAM pproximations. Using the three variables in equation (25), this interval was also produced from β at all orders M of homotopy approximation.

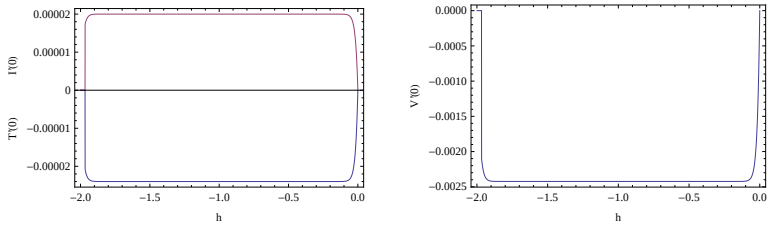

(a) $T'(0)$ and $I'(0)$ against h (b) $V'(0)$ against h

Figure 21: h-level curves for equation (25).

A proper definition of residual concerning the system (25) is given by (see also [9])

$$Res(h) = \int_0^{t_m} [g_1^2(t) + g_2^2(t) + g_3^2(t)]dt,$$

where

$$\begin{aligned} g_1 &= -T' + s - \mu_T T + rT\left(1 - \frac{T+I}{T_{max}}\right) - k_1 VT, \\ g_2 &= -I' + k_2 VT - \mu_1 I, \\ g_3 &= -V' + N\mu_b I - k_1 VT - \mu_V V. \end{aligned}$$

And further, dissimilar to the previous examples, the definition of ratio β is (see also [9])

$$\beta = \frac{1}{3}\left[\frac{||T_{k+1}(t)||}{||T_k(t)||} + \frac{||I_{k+1}(t)||}{||I_k(t)||} + \frac{||V_{k+1}(t)||}{||V_k(t)||}\right],$$

where the norm is assumed as L^2. The Res and β as computed above are shown in Figures 22 (a–b) from which the optimum value is $h \approx -0.592$, that is also the case from Table 12.

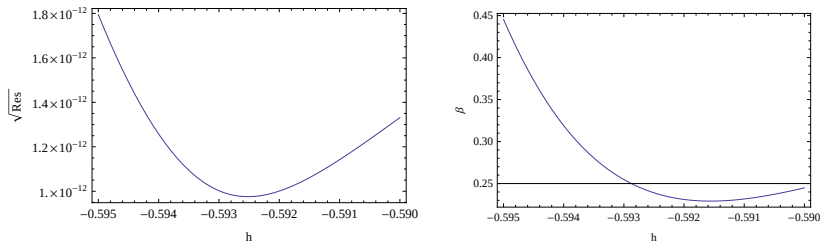

(a) The residual error (b) The ratio approach

Figure 22: The error $\sqrt{Res}$ and the ratio β regarding the problem (25) for the level of approximation $M = 60$.

The HAM approximation and its convergence for $h = -0.55$ regarding the present HIV model is justified in Table 13, see also Figure 23. Figures 24(a–c) are also drawn for $M = 60$ and $h = -0.59$.

3.8. Fornberg-Whitham partial differential equation

The Fornberg-Whitham partial differential equation has the form

$$\begin{aligned} u_t + u_x - u_{xxt} + uu_x - 3u_x u_{xx} - uu_{xxx} &= 0, \quad u(x,0) = e^{\frac{x}{2}}, \\ -1 \le x \le 1, \quad 0 \le t \le 1, \end{aligned} \tag{26}$$

M	h^{a}	CPU time	h^{b}	β	CPU time
10	−0.14111	10	−0.06616	0.90300	6
20	−0.47557	25	−0.68242	0.17599	13
30	−0.57105	42	−0.60757	0.02749	23
40	−0.59338	65	−0.59820	0.10422	34
50	−0.59136	101	−0.58948	0.26351	49
60	−0.59252	206	−0.59156	0.22911	91

Table 12: The values of optimal h, β and CPU times in seconds associated with (25) for various M. [a]Equation (8) and [b]Equation (12).

M	10	20	30	40	50	60
β	0.56265	0.86474	0.46861	0.43613	0.40424	0.38131

Table 13: The ratio β for $h = -0.55$ and approximation level $M = 60$.

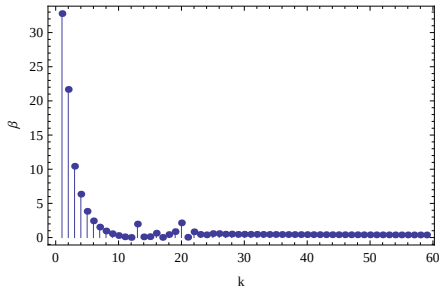

Figure 23: The ratio β for equation (25).

which has a type of traveling wave solution called a kink-like wave solution and it was used to study the qualitative behaviour of wave-breaking, see [15] and [17].

Substituting the auxiliary function and the auxiliary linear operator

$$H(x,t) = 1, \quad \mathcal{L} = \frac{\partial}{\partial t},$$

a few of the approximations of the homotopy series are

$$\begin{aligned}
u_1(x,t) &= -\frac{1}{2}e^{x/2}ht, \\
u_2(x,t) &= -\frac{1}{96}e^{x/2}ht\left(48 - 24h(3+t) + h^2\left(27 + 18t + 2t^2\right)\right), \\
u_3(x,t) &= \frac{1}{384}e^{x/2}ht\left(-192 + 144h(3+t) - 12h^2\left(27 + 18t + 2t^2\right) + h^3\left(81 + 81t + 18t^2 + t^3\right)\right), \\
&\vdots
\end{aligned}$$

To determine the interval of convergence, we define the norm

$$\|u(x,t)\| = \int_{-1}^{1}\int_{0}^{1} u^2(\zeta,\tau)d\tau d\zeta, \tag{27}$$

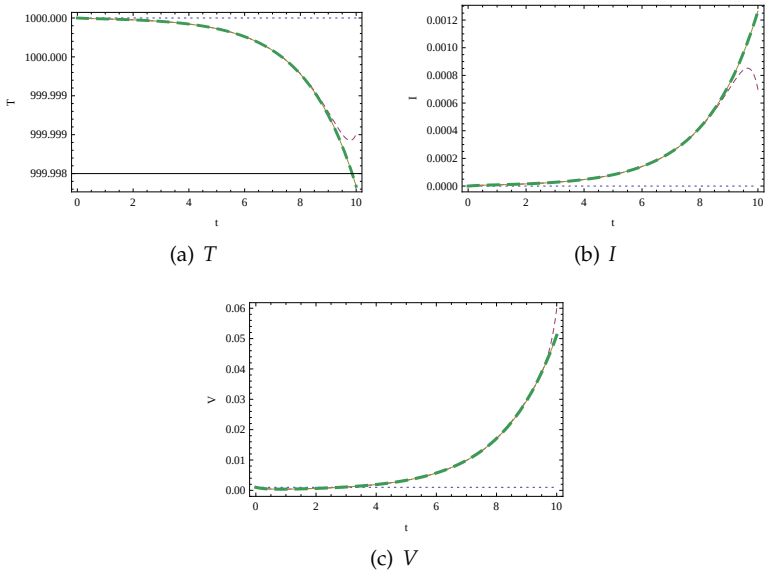

(a) T (b) I

(c) V

Figure 24: The HAM solutions for T, I and V with $h = -0.59$. Initial approximation (dotted curve), HAM approximation of 20th-order (dashed curve), HAM approximation of 60th-order (thick-dotted curve and exact solution (unbroken curve) for the system (25).

and enforce

$$\frac{\|u_{n+1}(x,t)\|}{\|u_n(x,t)\|} < 1.$$

Using this, the intervals of convergence at the iteration numbers $n = 6$, 10 and 20 result in

$$0 < h < 2.25552, \quad 0 < h < 2.31819, \quad 0 < h < 2.39624,$$

indicating that the Fornberg-Whitham equation (26) is convergent in a sufficiently large domain of h, without a need to display a $h-$curve as we did in previous examples.

In fact, a minimization process of the residual and ratio at the homotopy approximation level of $M = 20$ enables us to determine the values of optimal h as $h = 1.31$ (369 seconds CPU) and $h = 1.32$ (168 seconds CPU), respectively. At such optimal h, the residual is of order of magnitude 10^{-15} and the convergence is further assured by the ratio as demonstrated in Figure 25.

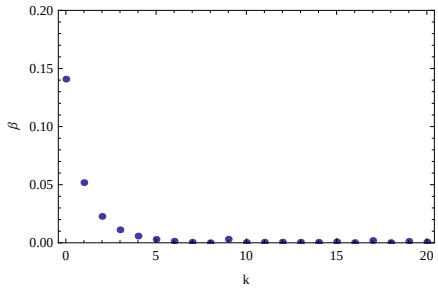

Figure 25: The ratio for equation (26).

Hence, this example proves that the presented ratio approach can be safely used to approximate the analytical solutions of partial differential equations of physical importance in the literature.

4. Concluding Remarks

The concept of the convergence control parameter employed in the homotopy analysis method (HAM) has been thoroughly revised in this paper following the recent book [9]. Distinct from the traditional notion of optimizing the squared residual error in an aim to get an optimal convergence control parameter, a new proposal is made here instead; obtaining an optimal convergence control parameter as a consequence of minimizing the successive ratios of the terms of the homotopy series for the considered physical problem at hand. The presented examples thoroughly indicate that the optimal convergence control parameters evaluated from the two approaches are almost equal for sufficiently large approximation orders. A variety of nonlinear algebraic, ordinary or partial differential equations have been used to verify the current ratio approach.

By means of the present ratio approach, the traditional h-level curves used to determine the value of h and its convergence interval are sorted out either exactly or numerically within less computational time. For some strongly nonlinear problems, whenever the full computation of squared residual is impossible, the new method still allows the calculation of ratios for the approximations levels of desire. The proposed ratio approach is particularly shown to be useful when the model involves an unknown parameter as in the plate oscillator problem of Von Karman and the eigenvalue problems.

We should mention here that as the minimum of squared residual, one can always calculate from the new approach the ratio of the homotopy terms even without ideas about the exact solution. Although not yet proved in terms of rigorous mathematics, surprisingly both methods generate the same convergence control parameters. Moreover, the present description has some advantages in terms of speed and exact evaluation of though integrals. After a rigorous proof that both techniques provide the same values for the convergence control, it is highly believed that the new technique may replace the classical squared residual method in the near future, at least all the highlighted physical examples point to this fact.

References

[1] R. V. Culshaw, S. Ruan, A delay-differential equation model of HIV infection of CD4+T-cells, Mathematical Biosciences 165 (200) 27–39.
[2] M. Ghoreishi, A. I. B. Md. Ismail, A. K. Alomari, Application of the homotopy analysis method for solving a model for HIV infection of CD4+ T-cells, Mathematical and Computer Modelling 54 (2011) 3007–3015.
[3] R. A. Van Gorder, K. Vajravelu, Analytic and numerical solutions to the Lane-Emden equation, Physics Letters A 372 (2006) 6060–6065.
[4] S. J. Liao, The proposed homotopy analysis technique for the solution of nonlinear problems, PhD thesis, Shanghai Jiao Tong University, 1992.
[5] S. J. Liao, Beyond perturbation: introduction to homotopy analysis method, Chapman & Hall/CRC, 2003.
[6] S. J. Liao, Notes on the homotopy analysis method: Some definitions and Theorems, Communications in Nonlinear Sciences and Numerical Simulations 14 (2009) 983–997.
[7] S. J. Liao. An optimal homotopy-analysis approach for strongly nonlinear differential equations, Communications in Nonlinear Sciences and Numerical Simulations 15 (2010) 2003–2016.
[8] S. J. Liao, Homotopy Analysis Method in Nonlinear Differential Equations, Springer-Verlag, 2012.
[9] S. J. Liao, Advances in the Homotopy Analysis Method, World Scientific, 2014.
[10] E. Magyari, I. Pop, B. Keller, Exact dual solutions occurring in Darcy mixed convection flow, International Journal of Heat and Mass Transfer, 44 (2001) 4563–4566.
[11] M. M. Rashidi, A. Shooshtari, O. Anwar Beg, Homotopy perturbation study of nonlinear vibration of Von Karman rectangular plates, Computers and Structures 106 (2012) 46–55.
[12] M. Turkyilmazoglu, Numerical and analytical solutions for the flow and heat transfer near the equator of an Mhd boundary layer over a porous rotating sphere, International Journal of Thermal Sciences, 50 (2011) 831–842.
[13] M. Turkyilmazoglu, The airy equation and its alternative analytic solution, Physica Scripta 86 (2012) 055004.
[14] M. Turkyilmazoglu, An effective approach for approximate analytical solutions of the damped Duffing equation, Physica Scripta 86 (2012) 015301.
[15] G. B. Whitham, Variational methods and applications to water wave, Proceedings of the Royal Society A 299 (1967) 6–25.
[16] K. Yabushita, M. Yamashita, K. Tsuboi, An analytic solution of projectile motion with the quadratic resistance law using homotopy analysis method, Journal of Physics A: Mathematical and Theoretical 40 (2007) 8403–8416.
[17] J. Zhou, L. Tian, A type of bounded traveling wave solutions for the Fornberg Whitham equation, Journal of Mathematical Analysis and Applications 346 (2008) 255–261.
[18] L. Zou, Z. Zong, G. H. Dong, Generalizing homotopy analysis method to solve Lotka-Volterra equation, Computers and Mathematics with Applications 56 (2008) 2289–2293.